Rice

Rice with Multilayer Aleurone: A Larger Sink for Multiple Micronutrients

Ronald Yu[1*†], Xiaoba Wu[1,3†], Jinxin Liu[3], Crispin A. Howitt[1], Anthony R. Bird[2], Chun-Ming Liu[3] and Philip J. Larkin[1*]

Abstract

Diet-related noncommunicable diseases impose a heavy burden on human health worldwide. Rice is a good target for diet-related disease prevention strategies because it is widely consumed. Liu et al. (Proc Natl Acad Sci USA 115(44):11327–11332, 2018. https://doi.org/10.1073/pnas.1806304115) demonstrated that increasing the number of cell layers and thickness of putative aleurone in *ta2-1* (*thick aleurone 2-1*) mutant rice enhances simultaneously the content of multiple micronutrients. However, the increases of aleurone-associated nutrients were not proportional to the increases in the aleurone thickness. In this study, first, cytohistological analyses and transmission electron microscopy demonstrated that the multilayer in *ta2-1* exhibited aleurone cell structural features. Second, we detected an increase in insoluble fibre and insoluble bound-phenolic compounds, a shift in aleurone-specific neutral non-starch polysaccharide profile, enhancement of phytate and minerals such as iron, zinc, potassium, magnesium, sulphur, and manganese, enrichment of triacylglycerol and phosphatidylcholine but slight reduction in free fatty acid, and an increase in oleic fatty acid composition. These findings support our hypothesis that the expanded aleurone-like layers in *ta2-1* maintained some of the distinctive aleurone features and composition. We provide perspectives to achieve even greater filling of this expanded micronutrient sink to provide a means for multiple micronutrient enhancements in rice.

Keywords: Aleurone bran, Fibre, Minerals, Multiple micronutrients, Nutrients, Phytate

Background

What We Know?

Globally, diet-related noncommunicable diseases (NCDs) have significant negative impacts on human health and create an ever-growing burden on health systems. According to the World Health Organization in 2014, chronic diseases such as cardiovascular diseases, cancers, and type II diabetes caused more than 63% of total deaths worldwide (Armstrong et al. 2014; GBD Risk Factors Collaborators 2016). Recognizing the compelling threat posed by NCDs, diet-related prevention strategies have become a top priority for all stakeholders with evident

social and economic advantages compared to efforts to cure these conditions (Lachat et al. 2013; World Health Organization 2005). The two central concepts behind the work presented here are that: (1) health outcomes can be achieved more readily by improving the composition of staple food; and (2) it is possible to co-ordinately improve multiple nutritional factors in order to achieve desired outcomes.

Rice represents an ideal target for such compositional intervention, being a widely consumed staple in both developing and developed countries. Among the top five most populated countries, China, India, and Indonesia are the developing countries that rely heavily on rice as a staple food (FAOSTAT 2019). White rice is the most commonly consumed type and a good source of dietary energy but poor in many essential nutrients including dietary fibre, antioxidants, phenolic

*Correspondence: Ronald.Yu@csiro.au; Phil.Larkin@csiro.au
†Ronald Yu and Xiaoba Wu contributed equally to this work.
[1] CSIRO Agriculture, GPO Box 1600, CSIRO, Building 801, CSIRO Black Mountain, Clunies Ross Street, Canberra, ACT 2601, Australia
Full list of author information is available at the end of the article

compounds, minerals, and vitamins. Improving the content of any one of these alone would likely be insufficient to reduce the risk of any specific type of chronic disease (Borresen and Ryan 2014; Henderson et al. 2012; Kahlon 2009; Nagendra Prasad et al. 2011). On the other hand, national campaigns have been initiated to promote brown rice (wholegrain rice) consumption. In the Philippines, a campaign called "BeRICEponsible" was initiated in 2014 to promote the health benefits associated with brown rice and to encourage brown rice consumption (Mohan et al. 2017). In comparison with white rice, brown rice is a good source of many essential nutrients because of the presence of aleurone in bran (mixed tissues of pericarp, testa, aleurone, and embryo).

In rice, the bran tissues provide about 40% of the total minerals, 90% of the total phosphorus, 50% of the total niacin (Vitamin B3), 50% of total lipid, and about 50% of the total phenolic compounds of the whole rice caryopsis (Goufo and Trindade 2014; Kik and Williams 1945; Resurreccion et al. 1979). Along with the embryo, aleurone is the major contributor to the micronutrients of bran, and the aleurone represents more than 66% of rice bran fraction (Taira 1995). Aleurone is the outermost cell layer of rice endosperm and very distinctive from the inner starchy endosperm (Becraft 2001; Wu et al. 2016). In rice, the number of aleurone layers can influence the quantities of important micronutrients such as iron and zinc (Sellappan et al. 2009; Yu et al. 2014). In our previous work we isolated and characterised in molecular genetic detail a rice mutant *thick aleurone 2-1* (*ta2-1*) with thicker aleurone phenotype; a point mutation in the 14th intron of the DNA demethylase *OsROS1* led to alternative splicing responsible for the new phenotype (Liu et al. 2018). In comparison with single-cell layer aleurone in the wild type, *ta2-1* has an average of 4.8 aleurone cell layers and up to 10 cell layers in some regions of the grain. Increases in nutritional components such as protein, lipid, starch, minerals, dietary fibre, antioxidants, and different vitamins were detected (Liu et al. 2018). However, the increases for most of the aleurone-associated nutrients and phytochemicals were not proportional to the increases in aleurone thickness. This was particularly evident for the important minerals of iron and zinc. This may suggest that the observed extra aleurone cells may not express the full biosynthetic functionality of aleurone cells, and/or the full allocation functionality of components such as iron and zinc. In the case of minerals, the uptake, transport and/or loading capacity may affect their final contents in aleurone.

What We Don't Know?

In this study, our aim is to test whether the multilayer aleurone in *ta2-1* maintains the various aleurone-like identities, and acts as a source for multiple nutritional enhancements. Two approaches were developed for this aim. First, different microscopic techniques were used to visualize the spatial and temporal distribution of different cellular and subcellular elements of aleurone cells in *ta2-1* during caryopsis development. Second, additional nutritional and compositional analyses were conducted to assess whether different nutritional elements such as dietary fibre and phenolic compounds, fatty acids, minerals, and phytate in the multi-layer aleurone of *ta2-1* follow the same aleurone-specific distribution patterns as in the wild-type. The interaction of minerals and phytate and their potential effect on human nutrition will be discussed. The aim of this study is to further improve the biofortification strategy in the *ta2-1* rice background and pave the way for similar improvements in other cereals.

Materials and Methods
Statistical Methods and Assumptions
Tukey's Honestly Significant Difference (Tukey's HSD) test was used to test the hypothesis that the nutrient content of *ta2-1* mutant rice was different from wild-type with the null hypothesis as no difference (Kirk 1968; Tukey 1953). Statistical analyses were conducted using R and all the results reported as significant were those with significance level of $P < 0.05$ (R Core Team 2013). The exact p-value of all the statistical analyses in this study can be found in the file of Figs. 5, 6, 7, 8, 9, 10, 11 and 12_RawData.xlsx in the supplementary information.

Cultivation of the Wild-Type and *ta2-1* Mutant Rice for Analysis
Rice mutant *ta2-1* was backcrossed three times (BC3) to remove unwanted ethyl methanesulfonate mutations, following by two rounds of self-pollination and selection to identify lines homozygous and stable for the thick-aleurone phenotype. The rice grains of BC3F3 homozygous *ta2-1* and wild-type Zhonghua 11 (ZH11) were sown side by side in the field for the grain increase in Haidian, Beijing, Peoples Republic of China (39.95°N, 116.38°E). In this study, 50 individual plants from *ta2-1* and wild-type ZH11 were harvested and analysed. The hull (palea and lemma) of the rice caryopsis was removed. No polishing was done so that the bran layer (including the rice aleurone layers) was maintained. Rice caryopses from 50 individual plants from *ta2-1* and wild-type were milled to wholegrain rice flour by Laboratory Mill 3100 (LM3100, Perten) in the same day and under similar temperature and humidity. This milled wholegrain rice flour sample was used for all the nutritional and biochemical analyses. This treatment has advantage that it can mimic the industrial milling procedure which requires a relatively large amount of rice caryopses as starting materials.

However, this treatment also results in a statistical limitation of low biological replicate. All the replicates used in my study represent technical replicates from one biological replicate of a single field trial. BC3F4 rice seed of *ta2-1* and ZH11 lines has been analysed in Liu et al. (2018) and BC3F5 seed was used for the current study.

Sudan Red Staining of Aleurone Tissue

Stain solution was prepared by dissolving 1 g of Sudan red IV in 50 ml of polyethylene glycol solution (202398, Sigma-Aldrich), incubated at 90 °C for one hour, and mixed with equal volume of 90% glycerol. After removing the fruit coat (palea and lemma) of each grain, mature rice grains were incubated in distilled water for five hours and then sectioned transversely or longitudinally using a razor blade. Sections were stained in Sudan red solution at room temperature for 24 to 72 h, followed by counterstaining with Lugol's staining solution (32922, Sigma-Aldrich) at room temperature for 20 min and observed under stereomicroscope (M80, Leica Microsystems) (Sreenivasulu et al. 2010).

Light Microscopic Observation Coupled with Calcofluor White or Periodic Acid-Schiff and Coomassie Brilliant Blue Staining

Rice grains were fixed in formalin-acetic acid-alcohol solution (60% ethanol, 5% glacial acetic acid and 2% formaldehyde), degassed for one hour, dehydrated in a series of alcohol solutions containing 70%, 80%, 95%, and 100% ethanol, infiltrated in LR white resin (14380, Electron Microscopy Sciences), and polymerized for 24 h at 60 °C. Microtome sectioning was done by Leica UC7 microtome (UC7, Leica Microsystems).

In Calcofluor white staining, sections were stained in 0.01% Calcofluor white solution (18909, Sigma-Aldrich) at room temperature for 2 min and examined by light microscopy.

In Periodic acid-Schiff (PAS) and Coomassie brilliant blue (CBB) staining, the fixed sections on slides were incubated in preheated 0.4% periodic acid (375810, Sigma-Aldrich) at 57 °C for 30 min, followed by rinsing in distilled water for three times. Schiff reagent (3952016, Sigma-Aldrich) was applied and the slides were incubated at room temperature for 15 min, following by rinsing three times in distilled water. The sections were then incubated in 1% Coomassie blue R-250 (20278, ThermoScientific) at room temperature for 2 min and rinsed three times with distilled water. Sections were dehydrated in a series of alcohol solutions of 30%, 50%, 60%, 75%, 85%, 95%, and 100% ethanol for 2 min each, followed by clearing of each slide in 50% xylene and 100% xylene solution (534056, Sigma-Aldrich) for 2 min each. The sections were then mounted on coverslips with Eukitt® quick hardening mounting medium (03989, Fluka) and observed under a light microscope.

Transmission Electron Microscopic Observation

After removing the fruit coat (palea and lemma) of each grain, mature rice grains were transversely sectioned by a razor blade. Sectioned rice grain was fixed in 2.5% glutaraldehyde in a 0.1 M sodium phosphate buffer (pH 7.0) for one hour, washed in the same buffer, and incubated at room temperature for 30 min for three times. The fixed rice grain was then undergone post-fixation in 1% osmium tetraoxide at 4 °C for 16 h (overnight). After fixation, samples were washed in sodium phosphate buffer (pH 7.0) for 30 min for three times, followed by dehydration in a series of alcohol solutions of 30%, 50%, 60%, 75%, 85%, 95%, and 100% ethanol for 10 min each. The dehydrated samples were then infiltrated with acetone and Spurr® solution (14300, Electron Microscopy Sciences) in a series of solutions with acetone to Spurr ratio of 1:0, 2:1, 1:1, 1:2, and 0:1 for four hours each, and embedded at 60 °C for 16 to 24 h. Embedded samples were sectioned, stained, and observed under transmission electron microscope (1230, JEOL), as reported by Roland and Vian (1991).

Aleurone Grain Measurement by Fiji ImageJ

TEM images were processed by the image processing package Fiji in ImageJ (Schindelin et al. 2012). In the Fiji package of ImageJ, the actual dimensions of TEM image were calibrated based on the scale bar, then threshold between 196 and 255 was selected to represent the aleurone grain area in wild type and *ta2-1*. Aleurone grain area was measured in terms of absolute area (μm^2) or percentage area to the whole image (%).

Total Mineral Content Estimation and Minerals Composition Measurement

The total mineral content of samples was measured by ash assay according to AOAC Method 923.03 (AOAC International 2016). In ash assay, about 2 g of desiccated rice flour was heated at 540 °C for 15 h and the mass of ash residue was then weighed.

Minerals composition was determined by ICP-OES (inductively coupled plasma optical emission spectrometry) (Zarcinas and Cartwright 1983; Zarcinas et al. 1987). In minerals composition assay, about 0.5 g of rice flour was digested using tube block digestion with 8 M nitric acid at 140 °C for eight hours. Zinc, iron, potassium, magnesium, phosphorus and sulphur content were then analysed using ICP-OES at CSIRO, Urrbrae, Adelaide, South Australia, at Waite Analytical Service (University of Adelaide, Waite, South Australia, Australia).

Total Phytic Acid Content

Determination of the phytate content of the flour samples was conducted based on the method of Harland and Oberleas (1986), as described in AOAC Method 986.11 (AOAC International 2016; Harland and Oberleas 1986). Briefly, 0.5 g cereal flour sample was weighed, extracted with 2.4% hydrochloric acid for one hour, and centrifuged. The supernatant was diluted and subjected to anion exchange column (500 mg, 59822065, Agilent Technologies) to remove the non-phytate elements. Phytate bound to the column was then eluted with 2 M hydrochloric acid. Phosphorous levels were determined by spectrophotometer using the molybdate and sulphonic acid colouring method with absorbance readings at 640 nm. Phytate was calculated using the following formula:

$$Phytate\ (mg/g) = Pconc * V1 * V2 / (1000 * sample\ weight * 0.282)$$

where P concentration is the concentration of phosphorous (μg/ml), as determined by spectrophotometry, V1 is the volume of the final solution, V2 is the volume of the extracted phytate solution, and 0.282 is the phosphorus to phytate conversion factor.

Fibre Content

Total dietary fibre was measured according to AOAC Method 985.29 and soluble and insoluble fibre according to AOAC Method 991.43 (AOAC International 2016).

Samples of 1 g of rice flour were undergone sequential enzymatic digestions of heat stable α-amylase (300 U/ml, E-BLAAM, Megazyme) and amyloglucosidase (3300 U/ml, E-AMGDF, Megazyme) to hydrolyse the starch content, followed by protease (350 tyrosine units/ml, E-BSPRT, Megazyme) to depolymerise the protein content. After the enzymatic digestions, different extraction and purification methods have applied to yield the total-, soluble- and insoluble-fibre fractions. Direct precipitation of sample after enzymatic digestions yielded the total-fibre; filtration of the enzymatic digested sample through Celite (61790-53-2, Sigma-Aldrich)-embedded fritted glass crucible, following by ethanol precipitation of the filtrate yielded the soluble-fibre while the residue after filtration represented the insoluble-fibre. After the enzymatic digestions and fibre extraction, the total-, soluble- and insoluble-dietary fibres were determined by the gravimetric measurements of the residue dry mass of the total-precipitated-residue, the filtrate-precipitated-residue and the residue after digestion respectively, with the correction from the parallel measurement of ash and protein content of the triplicate of each sample.

Total Neutral Non-starch Polysaccharide

Neutral non-starch polysaccharide (NNSP) was measured by the gas chromatographic procedure according to AOAC Method 994.13, as detailed by Theander et al. with slight modification (AOAC International 2016; Theander et al. 1995). Briefly, the total-dietary fibres extracted from total dietary fibre assay were hydrolysed with sulfuric acid. The neutral sugars released were then reduced by potassium borohydride solution and acetylated by acetic acids to alditol acetates, which are then quantified by gas chromatography. Gas chromatography conditions: BPX70 column (30 m x 320 μm × 0.25 μm); injection 0.5 μl; inlet at 240 °C; 20:1 split; 1.62 ml/min constant flow; oven at 180 °C for 2 min, 12 °C/min to 230 °C and hold for 8 min; flame ionization detector at 250 °C; quantification against internal allose standard.

Total Phenolic Compounds

Total phenols assay by FCR (Folin–Ciocalteu reagent) is an electron transfer-based assay, which estimates the amount of antioxidant based on the reducing power (willingness to donate electrons) of the antioxidants against oxidant probe molybdates, quantifies the reducing power with gallic acid standards, and presents as the value of gallic acid equivalents. Combined with the differential extractions of the free-, conjugated-, bound-, and total-fractions, FCR assay is good at determining the antioxidant capacity of different groups of phenolic compounds.

Total phenolic compounds content, as well as phenolic compounds in the free-, conjugated-, and bound-states were determined according to the method described by Li et al. with minor modifications (Li et al. 2008). Briefly, these four types of phenolic compounds were extracted from 100 mg samples with different extraction methods. Total-phenolic compounds were determined using 100 mg of samples, adding 200 μl 80% methanol, followed by alkaline hydrolysis with (2 M) sodium hydroxide; free-phenolic compounds were represented by the 80% methanol extraction of the 100 mg samples; conjugated-phenolic compounds were the alkaline hydrolysed products from the 80% methanol extract; bound-phenolic compounds were the alkaline hydrolysed products from the residues followed by the methanolic extraction of the free-phenolic compounds.

The amount of phenolic compounds in the treated/extracted samples was measured using FCR assay with reference to standard curve of known gallic acid concentrations. 1 ml of standards were added to 4 ml glass tubes. For test samples, 100 μl aliquots of thoroughly mixed samples were added to 900 μl water in 4 ml glass

tubes. 100 ml of FCR (F9252, Sigma-Aldrich) was then added to each tube and vortexed immediately. 700 μl sodium bicarbonate solution (1 M) was added after 2 min and mixed by vertexing. Each solution was incubated at room temperature in the dark for one hour. Absorbance was read at 765 nm. Results were expressed in μg gallic acid equivalents/g sample.

Folate Content

Total folate (Vitamin B9) was measured by commercially available VitaFast Folic acid kit (Folic Acid AOAC-RI, 100903, R-Biopharm) according to AOAC method 2004.05 as described by DeVries et al. (2005). The method incorporated the in vitro enzymes digestion and the growth response of the *Lactobacillus* to folate concentration in culture medium. First, pancreatin digestion was used for the release of the food matrix-bound folic acid. About 1 g of rice flour and 20 mg pancreatin were added and filled up to 40 ml with phosphate buffer (0.05 M, 0.1% ascorbate, pH7.2), and the sample was incubated at 37 °C for two hours in dark. These allowed the digestion of food matrix by protease and amylase in pancreatin and the hydrolyzation of polyglutamates to diglutamates by pancreatic conjugase to release food-bound folate which can be metabolized by *Lactobacillus*. After the incubation, the 1.5 ml reaction was centrifuged at 8000×*g* for 5 min, diluted to 10 ml with sterile distilled water, heated at 95 °C for 5 min, and filtered through a 0.2 μm filter to get rid of the insoluble or undigested suspensions in the sample. The filtrate was then diluted in several dilutions, added into the wells of a microtiter plate coated with *Lactobacillus casei* subspecies *rhamnosus*, and incubated at 37 °C for 44 to 48 h. After the incubation, the OD at 610–630 nm of the sample was measured and compared with the folate calibration standard. As the basal culture medium is lack of folate, the growth of the coated *Lactobacillus*, represented by the increase in turbidity of bacterial culture, is positively correlated with the extracted folate content in the sample. The folate concentration of the sample can be measured by comparing difference between the absorbance of the test sample with the calibration standards at OD 610–630 nm.

Total Lipid Content

Total lipid was measured according to AOAC Method 983.23 (AOAC International 2016). Sample of 5 g rice flour was incubated with 1% Clarase (MC23.31, Southern Biological) in 0.5 M sodium acetate solution at 45 °C for one hour. Lipids were extracted from the sample into chloroform/methanol by multiple extractions. The samples were then subjected to homogenization with multiple additions of chloroform/methanol. After centrifugation of the mixture into separate phases, the chloroform/methanol fraction was removed and dried at 101 °C for 30 min to recover the lipid. The total lipid in the sample was represented by the mass of residue after drying.

Triacylglycerol, Free Fatty Acid, and Phosphatidylcholine Fractionation and Quantification

According to the methodologies described by Liu et al., the extraction of total lipid, the fractionation of neutral lipid of mainly triacylglycerol (TAG), free fatty acid (FFA), and polar lipid of mainly phosphatidylcholine (PC), and the quantification of lipid were carried out (Liu et al. 2017). Thin layer chromatography (TLC) was first carried out to separate the neutral lipid and free fatty acid in solvent matrix of hexane:diethyl ether:acetic acid in 70:30:1 volume ratio. Then, another TLC was conducted in solvent matrix of chloroform:methanol:acetic acid:distilled water in 90:15:10:3 to separate the polar lipid PC. After TLC, samples were collected and lipid content in the fraction was extracted. The lipid fractions were undergone fatty acid methyl esters (FAME) and gas chromatography (GC) analyses and quantified according to the methods described by Vanhercke et al. (2014).

Total β-Glucan

Rice β-glucan was measured with reference to the methods in AOAC Method 995.16 (AOAC International 2016).

Briefly, 20 mg of rice flour were subjected to sequential enzymatic digestions of Lichenase and β-glucosidase, followed by quantification of the released glucose with standard glucose oxidase/peroxidase (GOPOD) system. Firstly, 200 μl 50% ethanol was added into 20 mg of rice flour, then 1 ml sodium phosphate buffer (20 mM, pH6.5) was added and incubated at 100 °C boiling water for 3 min. Secondly, the reaction was briefly cooled and diluted. Thirdly, 10 μl Lichenase (1U/μl) was added and incubated at 40 °C for 1 h. The sample was then diluted by adding 3.8 ml distilled water followed by centrifugation. Fourthly, the β-glucosidase reaction was conducted by adding 10 μl of β-glucosidase (2U/ml) into 10 μl sample supernatant collected in last step and incubated at 40 °C for 15 min.

Quantification of the glucose through GOPOD was conducted after the enzymatic reactions. Firstly, in 20 μl sample, 150 μl of glucose oxidase/peroxidase (GOPOD) reagent was added and incubated at 40 °C for 20 min. Secondly, the absorbance was measured at 510 nm for each sample (E_A) and reagent blank (E_{BLANK}). The β-glucan content was measured using the following formula:

$$\beta - \text{glucan} (\%\text{Weight/Total weight})$$
$$= \Delta E \times F \times 600 \times 1/1000 \times 100/W_d \times 162/180$$
$$= \Delta E/\Delta G/W_d \times 135$$

in which

$\Delta E =$ the difference between E_A and E_{BLANK}, F i = the absorbance of 2.5 μg of glucose, and $W_d =$ weight of sample analysed (in mg) times 0.86 ($W_d \times 0.86$).

Results

The Time Course of Aleurone Development in *ta2-1*

To compare the aleurone development in *ta2-1* and wild type, caryopses of 6, 8, 10, 12, 15, 18, 21, 24, and 30DAA (days after anthesis) were examined. These time points represent important developmental phases such as aleurone cell fate differentiation, aleurone nutrient accumulation, and aleurone maturation. These caryopses were sectioned and stained with Sudan red plus Lugol's iodine. The aleurone cells in *ta2-1* become prominent between 6 to 8DAA, being positively stained red by Sudan red (Fig. 1) indicating the dominance of lipid and almost complete absence of starch. Wild type had a thick aleurone resembling *ta2-1* up to 10DAA. From 12DAA onwards, *ta2-1* showed a thicker Sudan red staining area, although a slight decline of red staining area at 24 and 30DAA. Although there is no indication that starchy endosperm cells can become aleurone, it seems possible that some cell layers that initially show the compositional attributes of aleurone can become starchy endosperm in the later stages of development. In maize, *dek1* mutation triggered the transdifferentiation of the aleurone to starchy endosperm cells in the late stage of development (Becraft and Yi 2011). Furthermore, this switch is more pronounced in wild type caryopses than in *ta2-1*, leaving *ta2-1* with a thicker aleurone at maturity.

General Cell Structure of *ta2-1*

To assess the cellular and subcellular identities of aleurone cells in rice *ta2-1*, light microscopy coupled with two different staining methods were adopted.

Firstly, PAS-CBB staining, multiple layers of putative aleurone cells appeared distinctly different from starchy endosperm cells at the periphery of the mature rice caryopsis in *ta2-1*. The multiple layers of putative *ta2-1* aleurone cells had thicker cell walls (stained magenta by PAS) than the inner starchy endosperm cells (Fig. 2b, black arrow), prominent protein bodies (stained blue by CBB) (Fig. 2e, asterisk), and much lower starch granule density (Fig. 2f, g, black closed triangle). The putative aleurone cells in *ta2-1* were more irregular in shape than wild type aleurone cells, and with more and larger protein bodies. Moreover, their cell distribution patterns were different. In wild type, there was one aleurone layer on the ventral side (Fig. 2a) and up to five aleurone layers on the dorsal side of the rice caryopsis (Fig. 2c). In *ta2-1*, the aleurone layer was about three layers thick on the ventral side (Fig. 2b) and more than eight layers (Fig. 2d) on the dorsal side. Regarding the tissue organization, throughout the whole caryopses, *ta2-1* had more blue-stained aleurone-like area and less magenta-stained starchy-endosperm area than wild type (Fig. 2h, i). Between aleurone and starchy endosperm, protein bodies-rich sub-aleurone cell layer is present (Wu et al. 2016). In both *ta2-1* and wild type, heavily blue-stained sub-aleurone cell layers were observed (Fig. 2h, i, yellow oval). In the sub-aleurone cell layer, a mixture of lightly blue-stained aleurone cell, heavily blue-stained sub-aleurone cell, and magenta-stained starchy endosperm cell could present together (Fig. 2b).

Secondly, Calcofluor White staining was applied with epifluorescence microscopy to study the cell wall structure specifically. Calcofluor White binds to cellulose and
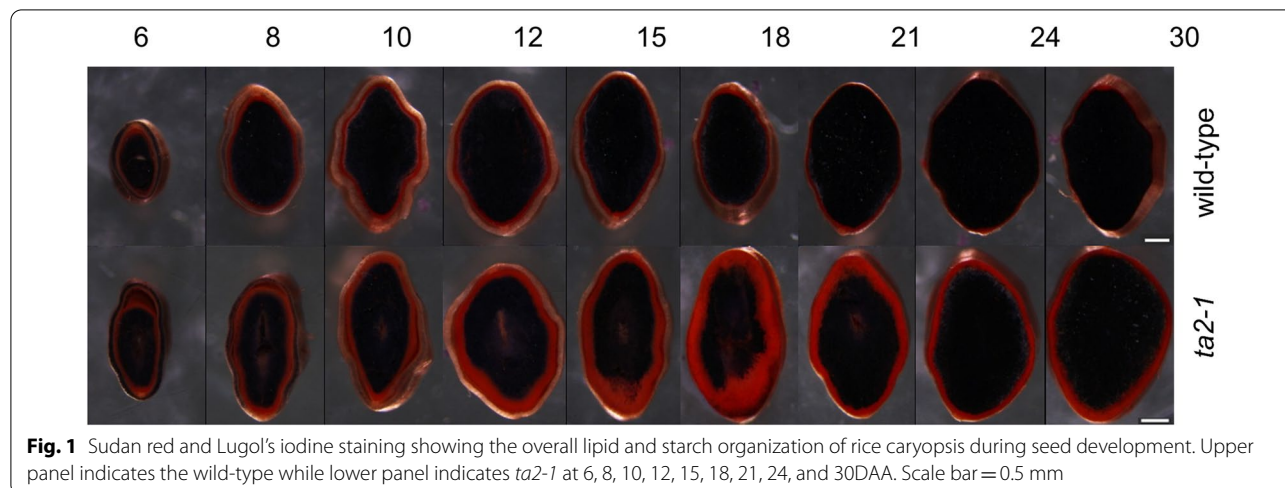

Fig. 1 Sudan red and Lugol's iodine staining showing the overall lipid and starch organization of rice caryopsis during seed development. Upper panel indicates the wild-type while lower panel indicates *ta2-1* at 6, 8, 10, 12, 15, 18, 21, 24, and 30DAA. Scale bar = 0.5 mm

other β-glucans in cell wall (Hughes and McCully 1975). In both wild type and *ta2-1*, the outermost compressed cells of the testa and the aleurone were actively stained while the innermost starchy endosperm cells were not (Fig. 3a, b). The putative extra aleurone layers of *ta2-1* resembled aleurone-like distinctive cell wall trait.

The Accumulation of Aleurone Grains in *ta2-1*

Transmission electron microscopy was used to examine the subcellular details of the putative aleurone cells in *ta2-1*. In both wild-type and *ta2-1* aleurone cells, thick cell walls were evident (Fig. 4a, b between two arrows). Also, protein bodies (sometimes referred to as aleurone grains (AG)) were abundant in both genotypes. As in the light microscopy study, AG in *ta2-1* were generally larger than the wild type with similar subcellular content. The *ta2-1* AG had other more subtle differences compared to wild type AG. Surrounded by tonoplast membrane, AG accumulate protein presumably as a source of amino acids for germination; they consist of three morphologically distinct features called the crystalloid, matrix, and globoid. These three features were present with similar electron density in the aleurone grains of both the wild type aleurone and the expanded *ta2-1* cells (Fig. 4c, e, arrows), however, the *ta2-1* AG were more variable in size with many being larger. When AG structures were selected and compared (Additional file 1: Fig. S1), 423.41μm^2 and 251.83μm^2 of AG area was observed in *ta2-1* and wild type respectively (Additional file 2: Table S1), suggesting that *ta2-1* had more AG area.

Together, the results from light microscopy and electron microscopy supported the conclusion that the putative extra aleurone cells in *ta2-1* retained the aleurone cell features of thick cell wall, low content of starch granules and presence of protein-rich AG. Distinctive AG features of crystalloid, matrix, and globoid were conserved in *ta2-1*. However, the *ta2-1* aleurone cells had a greater variability in cell size and shape of AG.

To measure the spatial distribution of aleurone cells, light microscopy coupled with PAS was adopted. From the outer to inner layers of the *ta2-1* aleurone, there was a change in structure and subcellular content of the AG. In wild type, only one type of AG was observed. The wild-type AG had a small internal cavity and abundant protein matrix that was stained deep blue by CBB. Moreover, individual aleurone cells were smaller in size (Fig. 2a, c) to those in *ta2-1* (Fig. 2b, d) The subcellular content and structure of the wild-type AG was uniform and constant. However, in *ta2-1*, two types of AG could be distinguished, i.e. AG with wild type morphology (Fig. 2e, f, single asterisk) and larger aleurone grains (LAG) (Fig. 2g, double asterisks). AG and LAG had similar deep-blue protein matrix feature, however, LAG had a larger internal globoid cavity with sometimes more limited protein matrix than AG. Moreover, the distribution patterns of LAG changed from outer to inner layers of the *ta2-1* aleurone. In the outer layers of *ta2-1* aleurone, the dominant storage compartment is AG while in inner layers, the dominant storage vacuoles resemble the LAG structure.

The Contents of Dietary Fibre, Phenolic Compounds, and Antioxidants

The aleurone cell wall in brown rice is an abundant source of dietary fibres. We previously showed that total dietary fibre content was increased in *ta2-1* (Liu et al. 2018). In this study, we compared the insoluble- and soluble- dietary fibre in the total fibre content of *ta2*-1. Similar to our previous findings, rice mutant *ta2-1* showed 66% increase in total dietary fibre. This was largely due to a 55% increase in insoluble-dietary fibre, while no significant change ($P = 0.90 > 0.05$) was observed in the content of soluble-dietary fibre (Fig. 5). Since it is known that the fibre associated with the aleurone cell wall is insoluble in nature (Collins et al. 2010), the observed increase in total and insoluble fibre in *ta2-1* is consistent with the thickened aleurone being the source of the extra fibre.

Dietary fibre is composed NNSP, nondigestible oligosaccharide, resistant starch, lignin, and uronic acid containing polysaccharides (Theander et al. 1995). Among

---

(See figure on next page.)

Fig. 2 PAS and CBB staining showing the subcellular cell content of the transverse section of the rice caryopsis. PAS binds to and stains carbohydrate magenta while CBB binds to and stains protein blue. Different types of cell present across the putative multiple-aleurone layers in *ta2-1*. **a** and **c** the overview of the wild-type aleurone layers on the ventral side (**a**) and dorsal side (**c**) of rice caryopsis; **b** and **d** the overview of the *ta2-1* aleurone layers on the ventral side (**b**) and dorsal side (**d**) of rice caryopsis; **e**–**g** the aleurone cells in the *ta2-1* outer (**e**), middle (**f**), and inner (**g**) multiplied cell layers in three different regions of **d**. **h** and **i** semi-thin transverse section of the rice caryopsis showing the aleurone and starchy endosperm tissue layers in wild type (**h**) and *ta2-1* (**i**). In **a**–**d**, black arrows indicate the cell wall. In **d**, black square indicates the locations to capture the images used in **e**–**g**. In **e**–**g**, a single asterisk indicates the protein body identified in *ta2-1* resembling wild-type structure. Double asterisks indicate the large protein body in *ta2-1*. Black closed triangle indicates the starch granules presented in the multiple aleurone layers of *ta2-1*. In **g**, **h**, white square indicates the estimated locations to capture the images used in **a** (ventral) and **b** (dorsal). Black square indicates the estimated locations to capture the images used in **b** (ventral) and **d** (dorsal). Yellow oval indicates the sub-aleurone layer. Scale bar for **a**–**g** = 10 μm. Scale bar for **h**, **i** = 0.5 mm
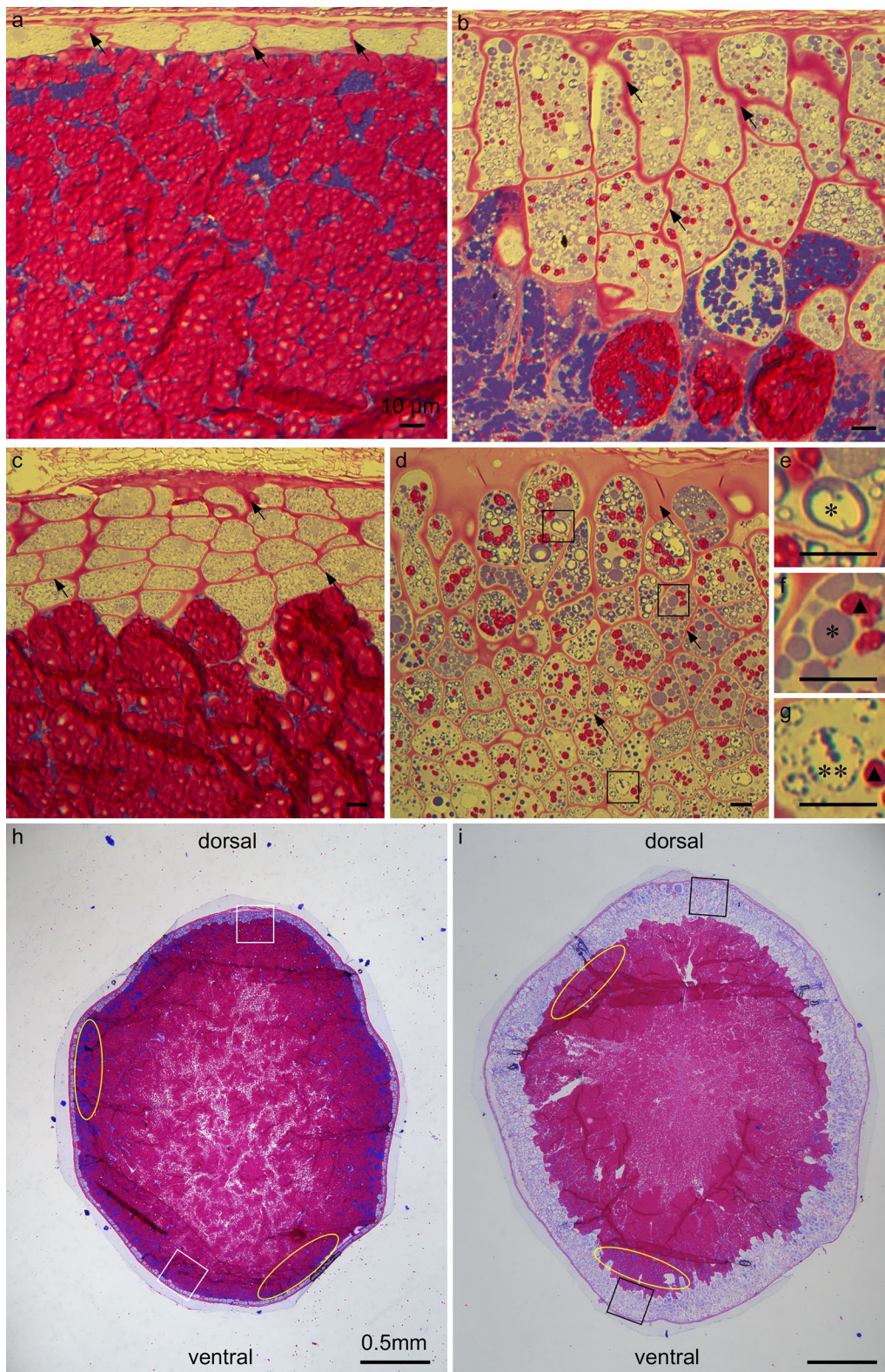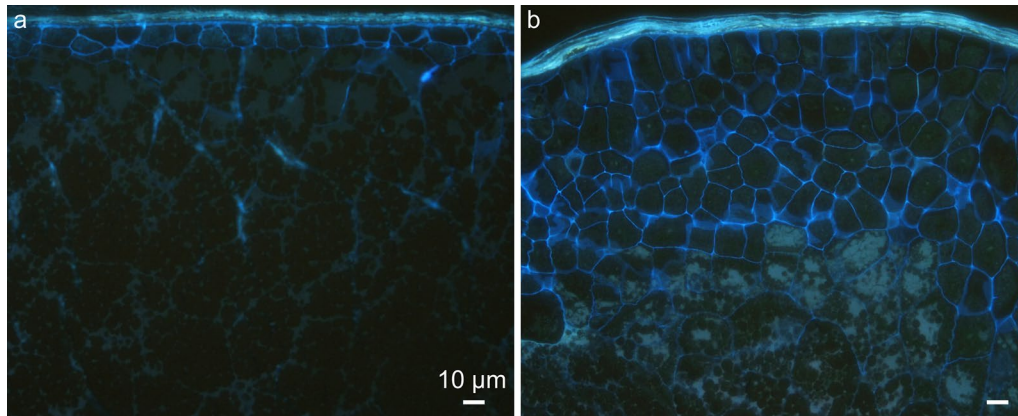
Fig. 2 (See legend on previous page.)

Fig. 3 Calcofluor White staining with epifluorescence showing the cell wall structure and organization of the transverse section of the rice caryopsis. **a** the wild type; **b** *ta2-1*. Scale bar = 10 μm
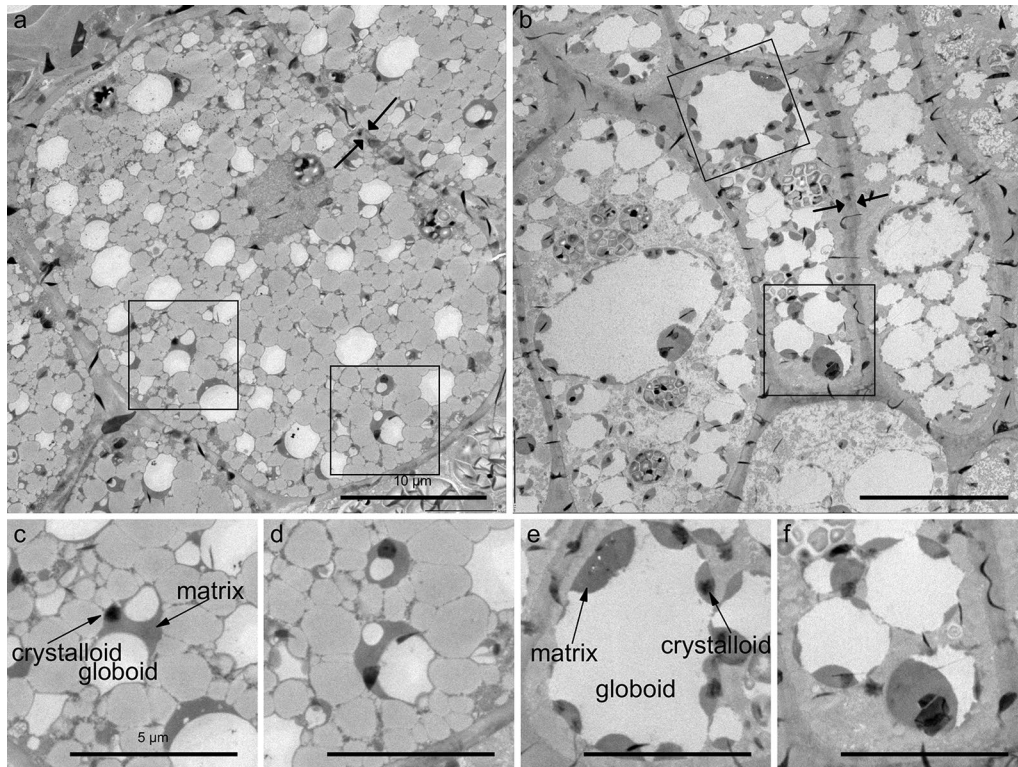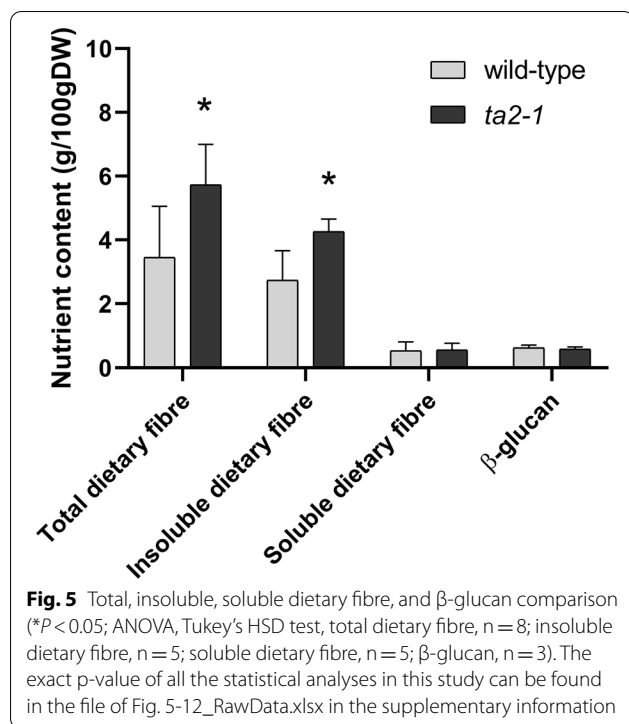

Fig. 4 Transmission electron microscopy (TEM) showing the aleurone cell structure of the transverse section of the rice caryopsis. **a** wild-type; **b** *ta2-1*. The thick cell wall is shown between the arrows and aleurone grains (AG) are selected with black square. **c**–**f** magnified images selected as AG; **c** and **d** wild-type AG; **e** and **f** *ta2-1* AG. Scale bar for **a** and **b** = 10 μm. Scale bar for **c**–**f** = 5 μm

these components, NNSP is the major contributor of the total dietary fibre content in rice caryopsis (Collins et al. 2010). The total NNSP content in the wholegrain flour of *ta2-1* was 61% higher than that in the wild-type (Fig. 6a). Moreover, being consistent with the earlier studies in different wholegrain (brown) rice varieties

(Collins et al. 2010; Demirbas 2005), the β-glucan content in the wild type and *ta2-1* was very low at 0.63 g and 0.59 g per 100 g respectively (Fig. 5). Aleurone is rich in arabinoxylan and low in cellulose and β-glucans, but starchy endosperm has an even distribution of these three fibre types (Fincher and Stone 2004). The

Fig. 5 Total, insoluble, soluble dietary fibre, and β-glucan comparison (*$P < 0.05$; ANOVA, Tukey's HSD test, total dietary fibre, n = 8; insoluble dietary fibre, n = 5; soluble dietary fibre, n = 5; β-glucan, n = 3). The exact p-value of all the statistical analyses in this study can be found in the file of Fig. 5-12_RawData.xlsx in the supplementary information

arabinose content increased from 18% in the wild type to 24% in *ta2-1*, and the xylose content from 17 to 20%; while glucose content dropped from 50% in the wild type to 40% in *ta2-1* (Fig. 6b), leading to changed NNSP composition profile in *ta2-1* (Fig. 6c). The basic monosaccharide units of arabinoxylan are arabinose and xylose, and the basic monosaccharide unit of cellulose and β-glucans is D-glucose. The increase in arabinose and xylose content at the expense of D-glucose in NNSP suggested that the expanded aleurone layers in *ta2-1* maintained the aleurone cell identity of arabinoxylan-rich cell wall and accounted for the composition change in total NNSP.

Antioxidants of rice include a wide spectrum of biomolecules such as phenolic compounds, uronic acids, tocopherols, carotenoids, ascorbic acid, and gamma-oryzanol which stabilize multiple oxidant sources and free radicals by their electron-transferring or hydrogen-transferring ability (Prior et al. 2005). Some antioxidants can be esterified and bound to the aleurone cell wall. Our previous studies focused on the electron-transferring ability of wholegrain rice flour through oxygen radical absorbance capacity (ORAC) and the hydrogen-transferring ability through FCR (Liu et al. 2018). Here we tested their association with the aleurone cell wall, by extracting antioxidant fractions with different solubility and measuring their hydrogen-transferring abilities.

Total-phenolic compounds in plants may exist in soluble free, soluble conjugated (esterified), and insoluble bound forms (Robbins 2003). The antioxidants were first extracted into the four fractions of total-, bound-, conjugated-, and free- phenolic compounds from the wholegrain rice flour samples. Their anti-oxidation abilities were then measured by the FCR assay. In both wild-type and *ta2-1*, about 80% of total phenolic compounds in rice caryopsis were insoluble bound-phenolic compounds, followed by 10% soluble free- and 10% soluble conjugated-phenolic compounds. Compared with the wild-type, *ta2-1* showed 35% increase in total-, 19% increase in insoluble bound-, no change in soluble free-, and 142% increase in soluble conjugated-phenolic compounds (Fig. 7). This pattern of increases is consistent with the increased aleurone thickness being responsible for the increased antioxidant capacity.
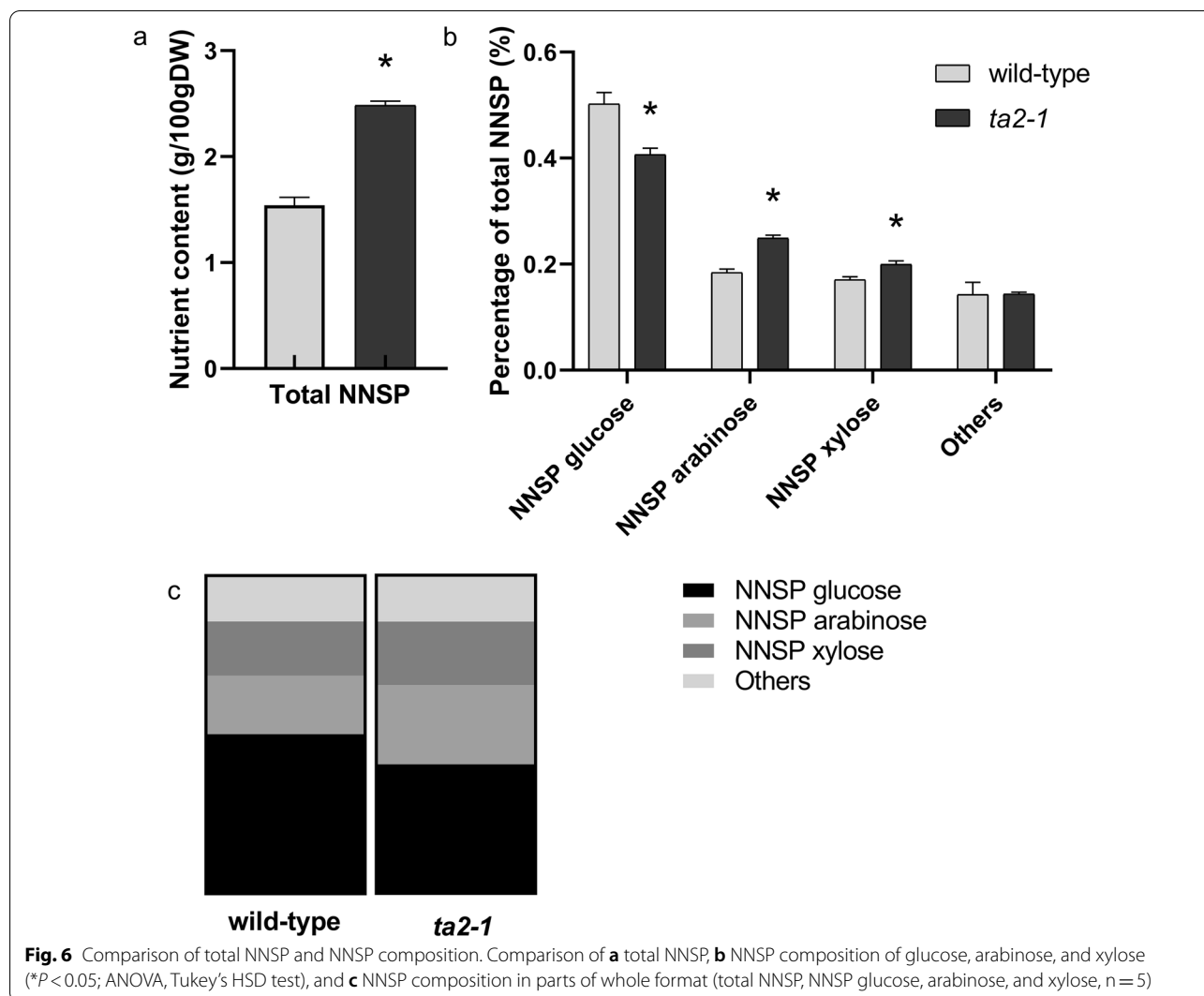
Folate (Vitamin B9) has potent antioxidant activity (Atteia et al. 2009). In rice, the aleurone-enriched bran fraction is rich in folate (Houston and Kohler 1970). In this study, compared with the wild-type, *ta2-1* had 32% increase in folate content (Fig. 8).

The Contents of Minerals and Phytate

Analyses of phytate and phosphorus content revealed increases of 18% and 22% respectively in *ta2-1* compared to wild type (Fig. 9). Assuming the molecular mass of phytate is 660.04gmol^{-1} and that of phosphorus is 30.97gmol^{-1} and each phytate molecular consists of six phosphorus molecules, 75.10% and 72.47% of total phosphorus are bound to phytate in wild type and *ta2-1* respectively (Additional file 3: Table S2). These measurements resemble the finding of others in rice caryopsis that 73.7% of total phosphorus content is bound to phytate (Ravindran et al. 1994). The similarity of percentage increase between phytate (18%) and phosphorus (22%) and the similar proportion of phosphorus bound to phytate suggested the increase of phosphorus in *ta2-1* is fully explained by the increase in phytate. Moreover, in addition to the increases in iron, zinc, and magnesium as observed by Liu et al. (2018), increases in manganese, potassium, and sulphur but not calcium content was observed (Fig. 10).

The Compositions and Contents of Lipid

It has been shown before that *ta2-1* mutant had higher total lipid content (Liu et al. 2018). The total oil content and composition in rice aleurone (rice bran) is different from starchy endosperm (Choudhury and Juliano 1980a, 1980b). These authors showed that the neutral lipids (largely TAG) were concentrated in the bran (embryo and aleurone), while the phospholipids were equally

Fig. 6 Comparison of total NNSP and NNSP composition. Comparison of **a** total NNSP, **b** NNSP composition of glucose, arabinose, and xylose (*$P < 0.05$; ANOVA, Tukey's HSD test), and **c** NNSP composition in parts of whole format (total NNSP, NNSP glucose, arabinose, and xylose, n = 5)
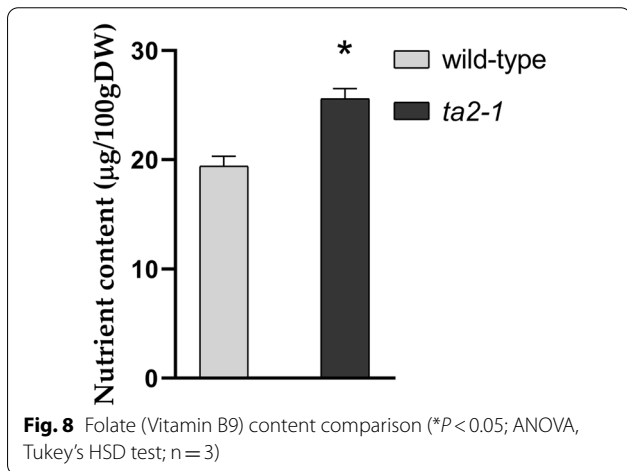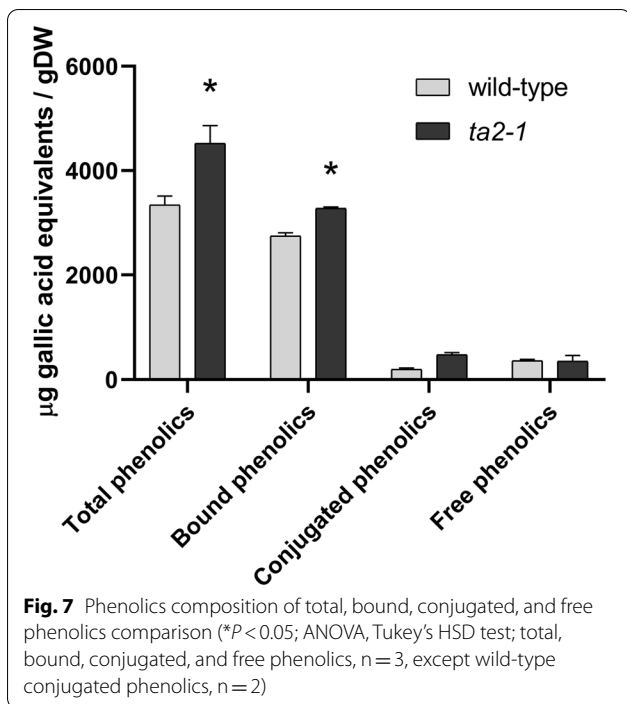
distributed in the bran and starchy endosperm fractions. In our studies, lipid components were separated using thin-layer chromatography and fatty acid content quantified by gas chromatography. In both *ta2-1* and wild type, TAG was the dominant type of lipid, followed by FFA, and PC. In comparison with wild type, *ta2-1* had a 79% increase in TAG (from 1.89 to 3.32%), 97% increase in PC (from 0.02390 to 0.04715%), and a 7% decrease in FFA (from 0.2171 to 0.2004%; not statistically significant) in wholegrain rice flour samples (Fig. 11). The large increase in TAG is expected if the thick aleurone is responsible for the increase in total lipid. There were changes in fatty acid profile in *ta2-1* (Fig. 12a), including 32% increase in oleic acid content (from 32 to 42% of the total fatty acid), 22% decrease in linoleic acid content (from 35 to 28%), and 5% decrease in palmitic acid content (from 17 to 16%) (Fig. 12b).

Discussion

General Aleurone Identity of the *ta2-1* Thick Aleurone

The aleurone cells in *ta2-1* maintained the aleurone-like features of thick cell wall, with few starch grains, an abundance of AG and lipid bodies, and as a consequence increases in dietary fibre, phenolic compounds, lipid composition, and changes to fatty acid profile matching what would be expected if the increases come from normal aleurone cells.

Cytohistology with Calcofluor white staining, cytohistology with PAS-CBB staining, and transmission electron microscopy all demonstrated a dramatic expansion of thick cell walls in the entire *ta2-1* aleurone. The AG in *ta2-1* aleurone cells were more abundant and had the same distinctive structures of crystalloid, matrix, and globoid as wild-type AG, however, they were more variable

Fig. 7 Phenolics composition of total, bound, conjugated, and free phenolics comparison (*$P < 0.05$; ANOVA, Tukey's HSD test; total, bound, conjugated, and free phenolics, n = 3, except wild-type conjugated phenolics, n = 2)

Fig. 9 Total phytate comparison by Harland and Oberleas method and total phosphorus comparison by ICP-OES (*$P < 0.05$; ANOVA, Tukey's HSD test; total phytate, n = 3; total phosphorus, n = 4)

Fig. 8 Folate (Vitamin B9) content comparison (*$P < 0.05$; ANOVA, Tukey's HSD test; n = 3)

in size with many being larger than in wild-type aleurone due mainly to larger globoid.

The increase in dietary fibre content in brown rice flours of *ta2-1* was mainly due to insoluble-dietary fibre, the type of fibre that forms aleurone cell walls (Collins et al. 2010). The increase in arabinose and xylose content in *ta2-1* flour and decrease in D-glucose was also consistent with the predominance of arabinoxylan in aleurone cell walls (Fincher and Stone 2004).
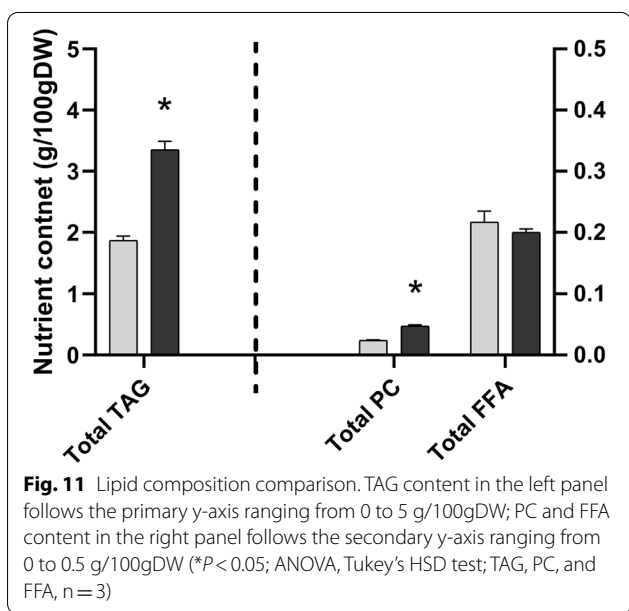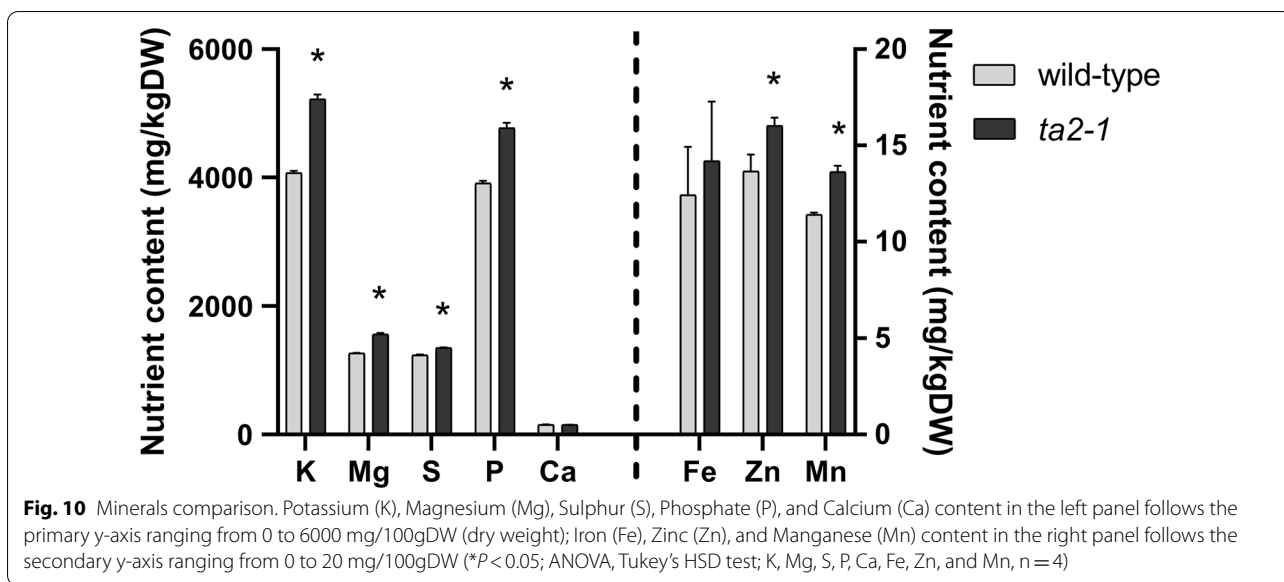
The enhanced thick cell wall in *ta2-1* also changes the phenolic compound composition. Associated with the cell wall are the phenolic compounds such as ferulic acid
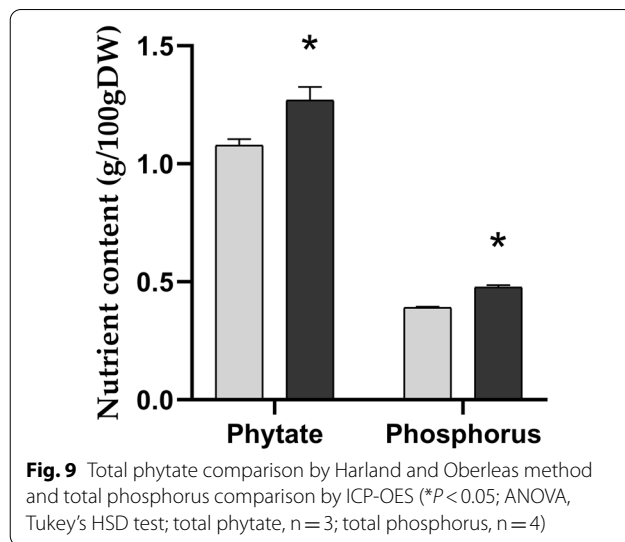
and ρ-coumaric acid. They are mainly bound to NNSP (Goufo and Trindade 2014). In *ta2-1*, the increase in total phenolic compounds was mainly attributable to an increase in insoluble bound-phenolic compounds.

Sudan red staining confirmed the enrichment of lipid bodies in the thickened *ta2-1* aleurone. The increase in TAG and PC in *ta2-1* flour but slight decrease in FFA, was consistent with a shift to aleurone- (bran-) specific lipid composition. Lipids in rice can be classified into non-starch lipids and starch-associated lipids (Zhou et al. 2003). Rice aleurone (bran) contributes to about 40% (39–41%) of total non-starch lipids that mainly consist of TAG and PC, while starchy endosperm stores about 60% (48–71%) of total starch-associated lipids with FFA as one of the major components (Choudhury and Juliano 1980a, 1980b). In *ta2-1* flour, the 79% increase in TAG, 97% increase in PC, and the 7% decrease in FFA is consistent with the thick aleurone maintaining normal aleurone cell function and composition. On the other hand, as the starchy endosperm content is reduced in *ta2-1*, the content of starch lipid FFA decreases.

The enrichment of lipid bodies in *ta2-1* aleurone also modifies the fatty acid profile. The fatty acid composition profiles of aleurone (bran) and starchy endosperm are different. Rice aleurone is rich in oleic acid (36% of total fatty acid) and linoleic (37%) but low in palmitic acid (23%) content. In starchy endosperm, linoleic and palmitic acid content are higher (41% and 33% respectively) but the oleic acid content is lower (20%) (Choudhury and Juliano 1980a, 1980b). The 32% increase in oleic, 22% decrease in linoleic, and 5% decrease in palmitic acid proportions again indicates that the multilayer aleurone in *ta2-1* maintains the aleurone-specific fatty acid profile.

Fig. 10 Minerals comparison. Potassium (K), Magnesium (Mg), Sulphur (S), Phosphate (P), and Calcium (Ca) content in the left panel follows the primary y-axis ranging from 0 to 6000 mg/100gDW (dry weight); Iron (Fe), Zinc (Zn), and Manganese (Mn) content in the right panel follows the secondary y-axis ranging from 0 to 20 mg/100gDW ($*P < 0.05$; ANOVA, Tukey's HSD test; K, Mg, S, P, Ca, Fe, Zn, and Mn, n = 4)

Fig. 11 Lipid composition comparison. TAG content in the left panel follows the primary y-axis ranging from 0 to 5 g/100gDW; PC and FFA content in the right panel follows the secondary y-axis ranging from 0 to 0.5 g/100gDW ($*P < 0.05$; ANOVA, Tukey's HSD test; TAG, PC, and FFA, n = 3)

Fig. 12 Fatty acid and fatty acid composition comparison. **a** Fatty acid composition comparison in parts of whole format, **b** Fatty acid composition comparison of oleic, linoleic, and palmitic acid ($*P < 0.05$; ANOVA, Tukey's HSD test; oleic, linoleic, and palmitic acid, n = 4)

Aleurone cells are rich in mitochondria (Jones 1969). In this study, no direct measurement of mitochondria was conducted, however, the folate content may be indicative of mitochondria abundance. Folate is enriched in aleurone-enriched bran fraction (Houston and Kohler 1970). In plant, folate is synthesized in three subcellular compartments in which the final five steps are conducted in mitochondria (Gorelova et al. 2017). About 30 – 50% of folate in cells is stored in mitochondria to help maintain the mitochondrial DNA stability (Depeint et al. 2006). Therefore, the 32% increase in folate may indirectly
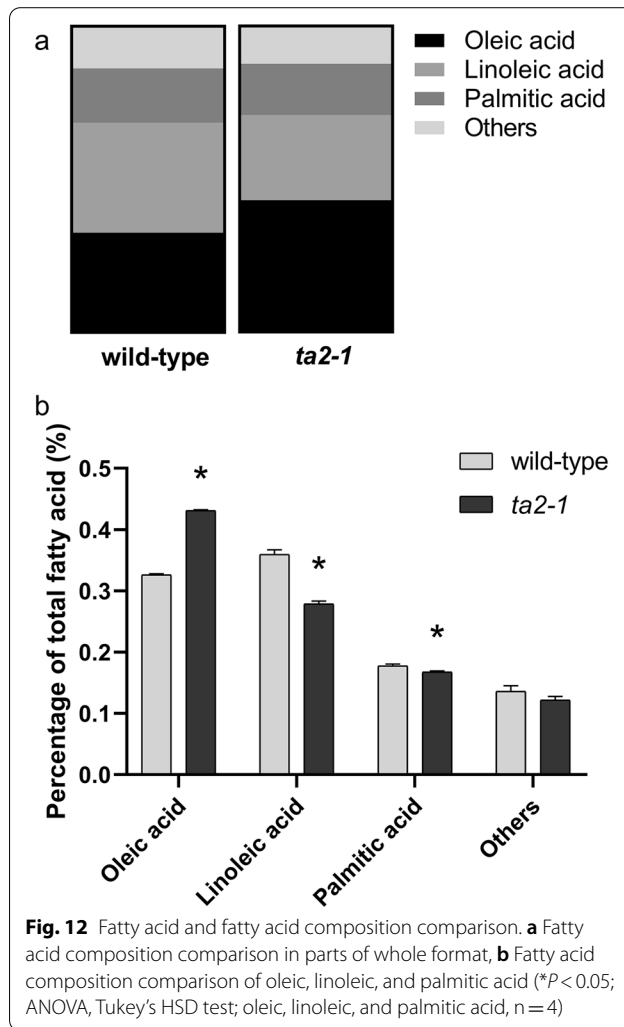
indicate that the multilayer aleurone in *ta2-1* maintains the aleurone-like high mitochondrial content.

Together, the cell structural features, the increase in insoluble fibre and insoluble bound-phenolic compounds, shift in aleurone-specific NNSP profile, enrichment of TAG and PC but slightly reduction in FFA and increase in oleic fatty acid composition collectively support the hypothesis that the additional aleurone-like layers in *ta2-1* maintain the distinctive features and composition of aleurone cells. It's the expansion of the aleurone layer that results in an increase of the nutrients that are associated with aleurone cell. However, these additional aleurone-like cells are irregular in cell size with larger globoid structure, which are different from wild-type aleurone cells.

The improvement of multiple nutritional factors in *ta2-1* can help prevention of NCDs. For example, dietary fibre can maintain gastrointestinal health by increasing fecal bulk, decreasing transit time, decreasing the gastrointestinal contact of foodborne carcinogenic compounds, binding to mutagens, and lowering colonic pH (Glitsø et al. 1998; Le Gall et al. 2009). The insoluble antioxidants bound to cell wall materials can provide an antioxidant environment contributing to protection of the colon tissues from cancer (Sengupta et al. 2001). Phytate has potential anti-neoplastic and antioxidant functions (Fox and Eberl 2002; Norhaizan et al. 2011). The multilayer aleurone rice with true aleurone composition can coordinately improve multiple nutritional factors to achieve diverse protective outcomes. In countries with rice-dominant diets, the consumption of wholegrain rice is very low (Cleveland et al. 2000; Harnack et al. 2003), but there is a growing trend from white rice to brown rice (with aleurone) consumption due to improved health consciousness and education (Selvam et al. 2017). By improving the nutrient composition of brown rice that is more readily accepted by the public, the multilayer aleurone rice *ta2-1* could therefore deliver substantial public health advantage without remarkably changing the dietary habits. Furthermore, light polishing of thick aleurone rice retains more aleurone than wild type rice and therefore also retains more of the nutrients.

The Commensurate Increase in Minerals and Phytate Content

Wholegrain flour of *ta2-1* had an 18% increase in phytate content. Using ICP-OES, we confirmed and extended our previous findings (Liu et al. 2018), showing *ta2-1* also had 14 to 23% increased content of various minerals.

Aleurone is a concentrated source of many essential minerals. In synchrotron X-ray fluorescence microscopy imaging study of rice, iron, zinc, manganese, and copper were highly concentrated in the aleurone layer (Hansen et al. 2012). Most of the minerals in rice are associated with phytate (Hansen et al. 2012; Mills et al. 2005; Simic et al. 2009). Wholegrain rice and wheat have similar phosphorus content (337 mg vs 323 mg/100gDW) (USDA 2020), however, rice has a higher proportion of phytate phosphorus than wheat, accounting for 77% of the total phosphorus content (Ravindran et al. 1994). Phytate has a strong affinity for chelating minerals such as Zn, Fe, and Mg, which limits their absorption in the small intestine (Bohn et al. 2007; Raboy 2009). This raises concern that phytate may impair small intestinal mineral absorption and compromise mineral status.

Wholegrain wheat flour has higher phytate and iron content than processed white flour, and in an in vitro *Caco-2* cells test, wholegrain wheat flour led to a lower ferritin response than processed white flour, suggesting that the iron content in white flour is more biologically available for cellular absorption and assimilation to ferritin (Eagling et al. 2014). Stevenson et al. summarized the findings in wheat and suggested that the consumption of wholegrain wheat or wheat bran decreased the calcium and zinc bioavailability (Stevenson et al. 2012).

However, the *Caco-2* test may not reveal the full picture concerning bioavailability. Diets high in whole grains do not adversely affect mineral nutrition but have favorable health outcomes. Different recommendations of daily wholegrain intake have been proposed in the U.S., Canada, and Australia, and no unfavourable health outcome has been reported regarding the high consumption of whole grains (Health Canada 2011; HHS & USDA 2015; National Health and Medical Research Council 2013). Recently, a meta-analysis provide further evidence that higher wholegrain consumption is associated with reduced risk of digestive tract cancers (Zhang et al. 2020). In both short-term (4 weeks) and long-term (2 years) studies in young and older women, the diet supplemented with phytate-rich wheat bran had no significant effect on different osteoporosis markers (Chen et al. 2004; Zittermann et al. 2007). Likewise, zinc absorption in young children was not negatively impacted by added phytate (Miller et al. 2015). Moreover, there is no consensus on the effect of phytate on iron bioavailability (Stevenson et al. 2012).

The digestion of phytate can happen in the human large intestine to release the chelated minerals for absorption. In pig studies, nearly complete (more than 97%) phytate digestion was observed in faecal samples following a normal diet with low intrinsic feed phytase (Schlemmer et al. 2001). In these studies, the highest phytate degradation occurred in the large intestine rather than the stomach or small intestine. In human faecal studies, the dietary phytate degradation rate varied between 50 and 90% (Joung et al. 2007; McCance and Widdowson 1935;

Walker et al. 1948). In a human trial with both young and elderly women, it was also reported that the diet with high phytate content could enhance phytate degradation (Joung et al. 2007). In the large intestine, the microbial phytases, foodborne phytases in plant food sources, and endogenous phytases can degrade cereal-grain phytate to release the minerals bound in the mineral-phytate inclusion for human absorption (Sandberg and Andlid 2002). Moreover, the fermentation of the NNSP and different dietary fibres in rice can potentially acidify the luminal environment of the large bowel (Koh et al. 2016). This can improve the mineral bioavailability. Therefore, the commensurate increments of minerals and phytate in *ta2-1* may not necessarily decrease the mineral availability; on the contrary, the increased phytate content in *ta2-1* may stimulate the microbial phytate degradation in large intestine, releasing bioavailable minerals and digested phytate for human absorption and gut microbiome development. However, more studies regarding the minerals' bioavailability should be conducted to further test this hypothesis.

Why are the Nutrient Increases Not Greater?

The increases in multiple nutrients in *ta2-1* flour are significant but not in proportion to the increased layers or volume of aleurone cells. We briefly explore here two hypotheses, which are not mutually exclusive, that might explain this "nutrient gap".

Hypothesis 1: The new larger aleurone may have a lower capacity to synthesize and/or store nutrients compared to wild-type aleurone.

While we have shown the expanded aleurone in *ta2-1* has the general features and composition of normal aleurone, there may be more subtle differences in biosynthetic or storage capacity. In rice, both wild-type and *ta2-1* aleurone cells have prominent AG. However, the AG in *ta2-1* aleurone cells are more variable in morphology and distribution pattern from outer to inner layers.

The rice *ta2-1* had two types of AG, morphologically normal AG and LAG. While both types of aleurone grains had prominent globoid, crystalloid, and matrix structures, LAGs in *ta2-1* had enlarged globoid cavities. The crystalloid is the storage compartment for the integral membrane proteins, whereas the matrix contains soluble protein (Jiang et al. 2002, 2000). The globoid is the mineral storage compartment consisting of mineral-phytate inclusion crystals. Studies from energy-dispersive X-ray analysis in rice and synchrotron soft X-ray microscopy in wheat suggested that minerals and phosphorus are co-localized with the globoid structures in the AG

(Ogawa et al. 1979; Regvar et al. 2011). However, during the sample preparation for transmission electron microscopy, the mineral-phytate crystals in the globoid can be easily dissolved out, thus leaving an electron-transparent internal globoid cavity in most of the electron microscopic analyses (Jacobsen et al. 1971). Despite these differences, some of the LAG in *ta2-1* accumulate protein that is stained by CBB, suggesting they are still functioning as storage compartments.

PAS and CBB staining also suggested that the distribution patterns of AG change from outer to inner layers of the *ta2-1* aleurone, with AG resembling wild-type structure in the outer layers, but LAG with empty or limited protein matrix predominant in the inner layers. The increased size of *ta2-1* aleurone cells and subcellular aleurone grains may signal a potential decrease in protein and mineral storage capacity from the outer to inner layers *ta2-1* aleurone.

Hypothesis 2: The aleurone development does not synchronize with the nutrient accumulation during grain development.

From 3-5DAA is the endosperm cellularization stage, during which cells at the periphery first take on distinguishable aleurone features. From 6-9DAA, the aleurone and starchy endosperm cells continue to divide and expand during the endosperm differentiation stage (Olsen et al. 2008; Wu et al. 2016). The proportion of aleurone tissue to starchy endosperm tissue is high in these early stages as compared with the mid and late grain developmental stages with limited cell division. This may explain why thick-aleurone was observed in both wild type and *ta2-1* up to 10DAA. Our histological analyses suggested that aleurone development in *ta2-1* occurs simultaneously with aleurone in the wild type throughout all phases of grain development, so it is likely biosynthetic activity and nutrient accumulation will be synchronized with the normal activities during grain development.

Of these hypotheses, the first appears to have relevance regarding nutrients synthesized in the aleurone, and requires further investigation.

Future Perspectives

The embryo is high in vitamin B1, vitamin E, and lipid, (Juliano 1993), so that any changes in embryo composition would also affect the overall wholegrain nutritional profile. Future studies should separate and study the composition of aleurone-, starchy endosperm-, and embryo- enriched fractions of *ta2-1*. It may also be possible to use synchrotron analysis to explore compositional

differences between the outer and inner layers of the *ta2-1* thick aleurone, especially in mineral accumulation.

Future studies should also focus on assessing the bioavailabilities of minerals in *ta2-1*. Various digestion models such as in vitro *Caco*-2 cell, in vivo animal feeding trial, and human intervention studies should be applied to measure their absorption efficiencies along the gastrointestinal tract.

Abbreviations
AG: Aleurone grain; BC3: Backcrossed three times; CBB: Coomassie brilliant blue; DAA: Days after anthesis; DW: Dry weight; FCR: Folin–Ciocalteu reagent; FFA: Free fatty acid; HSD: Honestly significant difference; LAG: Larger aleurone grains; NCD: Noncommunicable disease; NNSP: Neutral non-starch polysaccharide; ORAC: Oxygen radical absorbance capacity; PAS: Periodic acid-Schiff; PC: Phosphatidylcholine; *ta2-1*: *Thick-aleurone 2-1*; TAG: Triacylglycerol; TLC: Thin layer chromatography; ZH11: Zhonghua 11.

Supplementary Information
The online version contains supplementary material available at https://doi.org/10.1186/s12284-021-00543-3.

> **Additional file 1: Fig. S1**. Aleurone grain area comparison of TEM images. a: original image of wild-type in Fig. 4a; b: original image of ta2-1 in Fig. 4b. c and d: aleurone grain area was selected in red in wild type (c) and ta2-1 (d). Scale bar = 10μm.
>
> **Additional file 2: Table S1**. Aleurone grain area comparison of TEM images.
>
> **Additional file 3: Table S2**. Phosphorus content bound to phytate in rice wholegrain samples.

Authors' contributions
Conceptualization, CAH, ARB, CML, and PJL; methodology, JL, CAH, ARB, CML, and PJL; microscopic analysis, XW and JL; nutritional analysis, RY; statistical analysis and data visualization, RY; writing—original draft preparation, RY, XW, ARB, and PJL; writing—review and editing, XW, JL, CAH, ARB, CML, and PJL; supervision, CAH, ARB, CML, and PJL; project administration, CML and PJL; funding acquisition, CAH, ARB, CML, and PJL. All authors agree to this statement. All authors read and approved the final manuscript.

Availability of data and materials
The data generated or analysed during this study are included in (1) Supplementary information file in this article and (2) FigShare repository [https://figshare.com/s/0ae0f17be3bf75f2af4e] before publication. Once the manuscript has been accepted, public repository of [https://doi.org/10.6084/m9.figshare.12818867] will be available.

Declarations

Ethics approval and consent to participate
Not applicable.

Consent for publication
Not applicable.

Competing interests
RY, XW, JL, CAH, CML, and PJL are co-inventors on a patent for thick aleurone rice for which CSIRO and the Institute of Botany, Chinese Academy of Science are the co-owners.

Author details
[1]CSIRO Agriculture, GPO Box 1600, CSIRO, Building 801, CSIRO Black Mountain, Clunies Ross Street, Canberra, ACT 2601, Australia. [2]CSIRO Health and Biosecurity, PO Box 10041, Adelaide, SA 5000, Australia. [3]Key Laboratory of Plant Molecular Physiology, Institute of Botany, Chinese Academy of Sciences, Beijing, China.

References
AOAC International (2016) Official methods of analysis of AOAC International (Association of Official Analytical Chemists International ed.), 20th ed. AOAC, Gaithersburg

Armstrong T, Bettcher D, Branca F, Lauer J, Mace C, Mendis S, Poznyak V, Riley L, da Costa e Silva V, Stevens G (2014) Global status report on noncommunicable diseases 2014. World Health Organization Press, Geneva

Atteia BMR, El-Kak AA, Lucchesi PA, Delafontane P (2009) Antioxidant activity of folic acid: from mechanism of action to clinical application. FASEB J 23(S1):1. https://doi.org/10.1096/fasebj.23.1_supplement.103.7

National Health and Medical Research Council (2013) Australian dietary guidelines. Australia. www.nhmrc.gov.au/guidelines-publications/n55

Becraft PW (2001) Cell fate specification in the cereal endosperm. Semin Cell Dev Biol 12(5):387–394. https://doi.org/10.1006/scdb.2001.0268

Becraft PW, Yi G (2011) Regulation of aleurone development in cereal grains. J Exp Bot 62(5):1669–1675. https://doi.org/10.1093/jxb/erq372

Bohn L, Josefsen L, Meyer AS, Rasmussen SK (2007) Quantitative analysis of phytate globoids isolated from wheat bran and characterization of their sequential dephosphorylation by wheat phytase. J Agric Food Chem 55(18):7547–7552. https://doi.org/10.1021/jf071191t

Borresen EC, Ryan EP (2014) Rice bran: a food ingredient with global public health opportunities. Elsevier Inc, Pennsylvania

Chen Z, Stini WA, Marshall JR, Martinez ME, Guillen-Rodriguez JM, Roe D, Alberts DS (2004) Wheat bran fiber supplementation and bone loss among older people. Nutrition 20(9):747–751. https://doi.org/10.1016/j.nut.2004.05.015

Choudhury NH, Juliano BO (1980a) Effect of amylose content on the lipids of mature rice grain. Phytochemistry 19(7):1385–1389. https://doi.org/10.1016/0031-9422(80)80179-8

Choudhury NH, Juliano BO (1980b) Lipids in developing and mature rice grain. Phytochemistry 19(6):1063–1069. https://doi.org/10.1016/0031-9422(80)83057-3

Cleveland LE, Moshfegh AJ, Albertson AM, Goldman JD (2000) Dietary intake of whole grains. J Am Coll Nutr 19(3 Suppl):331S-338S

Collins HM, Burton RA, Topping DL, Liao ML, Bacic A, Fincher GB (2010) REVIEW: variability in fine structures of noncellulosic cell wall polysaccharides from cereal grains: potential importance in human health and nutrition. Cereal Chem 87(4):272–282. https://doi.org/10.1094/cchem-87-4-0272

Demirbas A (2005) beta-Glucan and mineral nutrient contents of cereals grown in Turkey. Food Chem 90(4):773–777. https://doi.org/10.1016/j.foodchem.2004.06.003

Depeint F, Bruce WR, Shangari N, Mehta R, O'Brien PJ (2006) Mitochondrial function and toxicity: role of B vitamins on the one-carbon transfer pathways. Chem Biol Interact 163:113–132. https://doi.org/10.1016/j.cbi.2006.05.010

DeVries JW, Rader JI, Keagy PM, Hudson CA, Angyal G, Arcot J, Castelli M, Doreanu N, Hudson C, Lawrence P, Martin J, Peace R, Rosner L, Strandler HS, Szpylka J, van den Berg H, Wo C, Wurz C (2005) Microbiological assay-trienzyme procedure for total folates in cereals and cereal foods: collaborative study. J AOAC Int 88(1):5–15

Eagling T, Wawer AA, Shewry PR, Zhao FJ, Fairweather-Tait SJ (2014) Iron bio-availability in two commercial cultivars of wheat: comparison between wholegrain and white flour and the effects of nicotianamine and 2'-deoxymugineic acid on iron uptake into Caco-2 cells. J Agric Food Chem 62(42):10320–10325. https://doi.org/10.1021/jf5026295

FAOSTAT (2019) Rice, paddy crop (production). http://www.fao.org/faostat/en/#data/QC

Fincher GB, Stone BA (2004) Chemistry of non-starch polysaccharides from cereal grains. In: Wrigley CW, Corke H, Walker CE (eds) Encyclopedia of grain science, vol 1. Elsevier Academic Press, Amsterdam

Fox CH, Eberl M (2002) Phytic acid (IP6), novel broad spectrum anti-neoplastic agent: a systematic review. Complement Ther Med 10(4):229–234. https://doi.org/10.1016/s0965-2299(02)00092-4

GBD Risk Factors Collaborators (2016) Global, regional, and national comparative risk assessment of 79 behavioural, environmental and occupational, and metabolic risks or clusters of risks, 1990–2015: a systematic analysis for the Global Burden of Disease Study 2015. Lancet 388:1659–1724. https://doi.org/10.1016/S0140-6736(16)31679-8

Glitsø LV, Brunsgaard G, Højsgaard S, Sandström B, Bach Knudsen KE (1998) Intestinal degradation in pigs of rye dietary fibre with different structural characteristics. Br J Nutr 80(5):457–468. https://doi.org/10.1017/S0007114598001536

Gorelova V, Ambach L, Rebeille F, Stove C, Van Der Straeten D (2017) Folates in plants: research advances and progress in crop biofortification. Front Chem 5:21. https://doi.org/10.3389/fchem.2017.00021

Goufo P, Trindade H (2014) Rice antioxidants: phenolic acids, flavonoids, anthocyanins, proanthocyanidins, tocopherols, tocotrienols, gamma-oryzanol, and phytic acid. Food Sci Nutr 2(2):75–104. https://doi.org/10.1002/fsn3.86

Hansen TH, Lombi E, Fitzgerald M, Laursen KH, Frydenvang J, Husted S, Boualaphanh C, Resurreccion A, Howard DL, de Jonge MD, Paterson D, Schjoerring JK (2012) Losses of essential mineral nutrients by polishing of rice differ among genotypes due to contrasting grain hardness and mineral distribution. J Cereal Sci 56(2):307–315. https://doi.org/10.1016/j.jcs.2012.07.002

Harland BF, Oberleas D (1986) Anion-exchange method for determination of phytate in foods: collaborative study. J Assoc Off Anal Chem 69(4):667–670

Harnack L, Walters SH, Jacobs DR (2003) Dietary intake and food sources of whole grains among US children and adolescents: data from the 1994–1996 continuing survey of food intakes by individuals. J Am Diet Assoc 103(8):1015–1019. https://doi.org/10.1016/S0002-8223(03)00470-X

Health Canada (2011) Eating well with Canada's food guide—a resource for educators and communicators. Canada. http://www.healthcanada.gc.ca/foodguide

Henderson AJ, Ollila CA, Kumar A, Borresen EC, Raina K, Agarwal R, Ryan EP (2012) Chemopreventive properties of dietary rice bran: current status and future prospects. Adv Nutr 3(5):643–653. https://doi.org/10.3945/an.112.002303

HHS & USDA (2015) 2015–2020 dietary guidelines for Americans. U.S. http://health.gov/dietaryguidelines/2015/guidelines/

Houston DF, Kohler GO (1970) Nutritional properties of rice. National Academy of Science, Washington

Hughes J, McCully ME (1975) The use of an optical brightener in the study of plant structure. Stain Technol 50(5):319–329. https://doi.org/10.3109/10520297509117082

Jacobsen JV, Knox RB, Pyliotis NA (1971) The structure and composition of aleurone grains in the barley aleurone layer. Planta 101:189–209

Jiang L, Phillips TE, Rogers SW, Rogers JC (2000) Biogenesis of the protein storage vacuole crystalloid. J Cell Biol 150(4):755–770. https://doi.org/10.1083/jcb.150.4.755

Jiang L, Erickson A, Rogers J (2002) Multivesicular bodies: a mechanism to package lytic and storage functions in one organelle? Trends Cell Biol 12(8):362–367. https://doi.org/10.1016/s0962-8924(02)02322-x

Jones RL (1969) The fine structure of barley aleurone cells. Planta 85:359–375

Joung H, Jeun BY, Li SJ, Kim J, Woodhouse LR, King JC, Welch RM, Paik HY (2007) Fecal phytate excretion varies with dietary phytate and age in women. J Am Coll Nutr 26(3):295–302. https://doi.org/10.1080/07315724.2007.10719614

Juliano BO (1993) Grain structure, composition and consumers criteria for quality. In: Lupien JR (ed) Rice in human nutrition. FAO, IRRI, Rome, pp 35–60

Kahlon TS (2009) Rice bran: production, composition, functionality and food applications, physiological benefits. In: Cho SS, Samuel P (eds) Fiber ingredients food applications and health benefits. CRC Press, Boca Raton, pp 305–321

Kik MC, Williams RR (1945) The nutritional improvement of white rice. Natl Res Council Bull 112:23–25

Kirk RE (1968) Experimental design: procedures for the behavioral sciences. Brooks-Cole Publishing, Belmont

Koh A, De Vadder F, Kovatcheva-Datchary P, Backhed F (2016) From dietary fiber to host physiology: short-chain fatty acids as key bacterial metabolites. Cell 165(6):1332–1345. https://doi.org/10.1016/j.cell.2016.05.041

Lachat C, Otchere S, Roberfroid D, Abdulai A, Seret FM, Milesevic J, Xuereb G, Candeias V, Kolsteren P (2013) Diet and physical activity for the prevention of noncommunicable diseases in low- and middle-income countries: a systematic policy review. PLoS Med 10(6):e1001465. https://doi.org/10.1371/journal.pmed.1001465

Le Gall M, Serena A, Jørgensen H, Theil PK, Bach Knudsen KE (2009) The role of whole-wheat grain and wheat and rye ingredients on the digestion and fermentation processes in the gut—a model experiment with pigs. Br J Nutr 102(11):1590–1600. https://doi.org/10.1017/S0007114509990924

Li L, Shewry PR, Ward JL (2008) Phenolic acids in wheat varieties in the HEALTHGRAIN diversity screen. J Agric Food Chem 56(21):9732–9739. https://doi.org/10.1021/jf801069s

Liu Q, Guo Q, Akbar S, Zhi Y, El Tahchy A, Mitchell M, Li Z, Shrestha P, Vanhercke T, Ral JP, Liang G, Wang MB, White R, Larkin P, Singh S, Petrie J (2017) Genetic enhancement of oil content in potato tuber (*Solanum tuberosum* L.) through an integrated metabolic engineering strategy. Plant Biotechnol J 15(1):56–67. https://doi.org/10.1111/pbi.12590

Liu J, Wu X, Yao X, Yu R, Larkin PJ, Liu CM (2018) Mutations in the DNA demethylase *OsROS1* result in a thickened aleurone and improved nutritional value in rice grains. Proc Natl Acad Sci USA 115(44):11327–11332. https://doi.org/10.1073/pnas.1806304115

McCance RA, Widdowson EM (1935) Phytin in human nutrition. Biochem J 29(12):2694–2699. https://doi.org/10.1042/bj0292694

Miller LV, Hambidge KM, Krebs NF (2015) Zinc absorption is not related to dietary phytate intake in infants and young children based on modeling combined data from multiple studies. J Nutr 145(8):1763–1769. https://doi.org/10.3945/jn.115.213074

Mills ENC, Parker ML, Wellner N, Toole G, Feeney K, Shewry PR (2005) Chemical imaging: the distribution of ions and molecules in developing and mature wheat grain. J Cereal Sci 41(2):193–201. https://doi.org/10.1016/j.jcs.2004.09.003

Mohan V, Ruchi V, Gayathri R, Ramya Bai M, Shobana S, Anjana RM, Unnikrishnan R, Sudha V (2017) Hurdles in brown rice consumption. In: Manickavasagan A, Santhakumar C, Venkatachalapathy N (eds) Brown rice. Springer, Cham, pp 255–270

Nagendra Prasad MN, Sanjay KR, Shravya Khatokar M, Vismaya MN, Nanjunda Swamy S (2011) Health benefits of rice bran: a review. J Nutr Food Sci 01(03):1000108. https://doi.org/10.4172/2155-9600.1000108

Norhaizan ME, Norashareena MS, Abdah MA (2011) Antioxidant and cytotoxicity effect of rice bran phytic acid as an anticancer agent on ovarian, breast and liver cancer cell lines. Malays J Nutr 17:367–375

Ogawa M, Tanaka K, Kasai Z (1979) Energy-dispersive x-ray analysis of phytin globoids in aleurone particlees of developing rice grains. Soil Sci Plant Nutr 25:437–448

Olsen OA, Potter RH, Kalla R (2008) Histo-differentiation and molecular biology of developing cereal endosperm. Seed Sci Res 2(3):117–131. https://doi.org/10.1017/s0960258500001240

Prior RL, Wu X, Schaich K (2005) Standardized methods for the determination of antioxidant capacity and phenolics in foods and dietary supplements. J Agric Food Chem 53(10):4290–4302. https://doi.org/10.1021/jf0502698

R Core Team (2013) R: a language and environment for statistical computing. R Foundation for Statistical Computing, Vienna. http://www.R-project.org/

Raboy V (2009) Approaches and challenges to engineering seed phytate and total phosphorus. Plant Sci 177(4):281–296. https://doi.org/10.1016/j.plantsci.2009.06.012

Ravindran V, Ravindran G, Sivalogan S (1994) Total and phytate phosphorus contents of various foods and feedstuffs of plant-origin. Food Chem 50(2):133–136. https://doi.org/10.1016/0308-8146(94)90109-0

Regvar M, Eichert D, Kaulich B, Gianoncelli A, Pongrac P, Vogel-Mikus K, Kreft I (2011) New insights into globoids of protein storage vacuoles in wheat aleurone using synchrotron soft X-ray microscopy. J Exp Bot 62(11):3929–3939. https://doi.org/10.1093/jxb/err090

Resurreccion AP, Juliano BO, Tanaka Y (1979) Nutrient content and distribution in milling fractions of rice grain. J Sci Food Agric 30(5):475–481. https://doi.org/10.1002/jsfa.2740300506

Robbins RJ (2003) Phenolic acids in foods: an overview of analytical methodology. J Agric Food Chem 51(10):2866–2887. https://doi.org/10.1021/jf026182t

Roland JC, Vian B (1991) General preparation and staining of thin sections. In: Hall JH, Hawes C (eds) Electron microscopy of plant cells. Academic Press, London, pp 1–66

Sandberg AS, Andlid T (2002) Phytogenic and microbial phytases in human nutrition. Int J Food Sci Technol 37(7):823–833. https://doi.org/10.1046/j.1365-2621.2002.00641.x

Schindelin J, Arganda-Carreras I, Frise E, Kaynig V, Longair M, Pietzsch T, Preibisch S, Rueden C, Saalfeld S, Schmid B, Tinevez JY, White DJ, Hartenstein V, Eliceiri K, Tomancak P, Cardona A (2012) Fiji: an open-source platform for biological-image analysis. Nat Methods 9(7):676–682. https://doi.org/10.1038/nmeth.2019

Schlemmer U, Jany KD, Berk A, Schulz E, Rechkemmer G (2001) Degradation of phytate in the gut of pigs–pathway of gastro-intestinal inositol phosphate hydrolysis and enzymes involved. Arch Tierernahr 55(4):255–280. https://doi.org/10.1080/17450390109386197

Sellappan K, Datta K, Parkhi V, Datta SK (2009) Rice caryopsis structure in relation to distribution of micronutrients (iron, zinc, β-carotene) of rice cultivars including transgenic indica rice. Plant Sci 177(6):557–562. https://doi.org/10.1016/j.plantsci.2009.07.004

Selvam S, Masilamani P, Umashankar PT, Alex Albert V (2017) Opportunities and challenges in marketing of brown rice. In: Manickavasagan A, Santhakumar C, Venkatachalapathy N (eds) Brown rice. Springer International Publishing, Cham, pp 271–282

Sengupta S, Tjandra JJ, Gibson PR (2001) Dietary fiber and colorectal neoplasia. Dis Colon Rectum 44:1016–1033

Simic D, Sudar R, Ledencan T, Jambrovic A, Zdunic Z, Brkic I, Kovacevic V (2009) Genetic variation of bioavailable iron and zinc in grain of a maize population. J Cereal Sci 50(3):392–397. https://doi.org/10.1016/j.jcs.2009.06.014

Sreenivasulu N, Borisjuk L, Junker BH, Mock HP, Rolletschek H, Seiffert U, Weschke W, Wobus U (2010) Barley grain development toward an integrative view. Int Rev Cell Mol Biol 281:49–89. https://doi.org/10.1016/S1937-6448(10)81002-0

Stevenson L, Phillips F, O'Sullivan K, Walton J (2012) Wheat bran: its composition and benefits to health, a European perspective. Int J Food Sci Nutr 63(8):1001–1013. https://doi.org/10.3109/09637486.2012.687366

Taira H (1995) Physicochemical properties and quality of rice grains. In: Matsuo T, Kumazawa K, Ishii R, Ishihara K, Hirata H (eds) Science of the rice plant, vol 2. Food and Agriculture Policy Research Center, Tokyo, p 1073

Theander O, Aman P, Westerlund E, Andersson R, Pettersson D (1995) Total dietary fiber determination as neutral sugar residues, uronic acids, and Klason lignin (the Uppsala method): collaborative study. J AOAC Int 78(4):1030–1044

Tukey JW (1953) The problem of multiple comparisons. Unpublished report. Princeton University, Princeton

USDA (2020) USDA food composition database. U.S. Department of Agriculture. Retrieved 2021. https://www.nal.usda.gov/usda-food-composition-database

Vanhercke T, El Tahchy A, Liu Q, Zhou XR, Shrestha P, Divi UK, Ral JP, Mansour MP, Nichols PD, James CN, Horn PJ, Chapman KD, Beaudoin F, Ruiz-Lopez N, Larkin PJ, de Feyter RC, Singh SP, Petrie JR (2014) Metabolic engineering of biomass for high energy density: oilseed-like triacylglycerol yields from plant leaves. Plant Biotechnol J 12(2):231–239. https://doi.org/10.1111/pbi.12131

Walker ARP, Fox FW, Irving JT (1948) Studies in human mineral metabolism. 1. The effect of bread rich in phytate phosphorus on the metabolism of certain mineral salts with special reference to calcium. Biochem J 42(3):452–462. https://doi.org/10.1042/bj0420452

World Health Organization (2005) Preventing chronic diseases: a vital investment. In: Vita-Finz L (eds) WHO global report. WHO Press, World Health Organization, Geneva

Wu X, Liu J, Li D, Liu CM (2016) Rice caryopsis development II: dynamic changes in the endosperm. J Integr Plant Biol 58(9):786–798. https://doi.org/10.1111/jipb.12488

Yu X, Zhou L, Xiong F, Wang Z (2014) Structural and histochemical characterization of developing rice caryopsis. Rice Sci 21(3):142–149. https://doi.org/10.1016/s1672-6308(13)60176-6

Zarcinas BA, Cartwright B (1983) Analysis of soil and plant material by inductively coupled plasma-optical emission spectrometry. C. Publishing (ed), vol 45. CSIRO, Australia

Zarcinas BA, Cartwright B, Spouncer LR (1987) Nitric acid digestion and multi-element analysis of plant material by inductively coupled plasma spectrometry. Commun Soil Sci Plant Anal 18:131–146

Zhang XF, Wang XK, Tang YJ, Guan XX, Guo Y, Fan JM, Cui LL (2020) Association of whole grains intake and the risk of digestive tract cancer: a systematic review and meta-analysis. Nutr J 19(1):52. https://doi.org/10.1186/s12937-020-00556-6

Zhou ZK, Blanchard C, Helliwell S, Robards K (2003) Fatty acid composition of three rice varieties following storage. J Cereal Sci 37(3):327–335. https://doi.org/10.1006/jcrs.2002.0502

Zittermann A, Scheld K, Danz A, Stehle P (2007) Wheat bran supplementation does not affect biochemical markers of bone turnover in young adult women with recommended calcium intake. Br J Nutr 82(6):431–435. https://doi.org/10.1017/s0007114599001683

Publisher's Note